High energy electrons

Power law spectra observed in many types of objects

Cosmic rays
Diffuse emission from the ISM
Supernovae
Supernova remnants
Pulsars
Normal galaxies
Jets from AGNs
Compact radio sources in AGNs
Gamma-ray bursts
.....

Synchrotron emission

$$\frac{dn}{dE} \propto \frac{dn}{d\gamma} \propto E^{-p} \propto \gamma^{-p}$$

$$j(\nu) \propto B^2 \int \gamma^2 \delta(\nu - \gamma^2 \nu_B) \gamma^{-p} d\gamma \propto B^{(p+1)/2} \nu^{-(p-1)/2}$$

$$\nu_B = 4.2 \times 10^6 B(G) \quad Hz$$

$$\nu_c = \frac{eB}{2\pi m_e c} \gamma^2 = 4.2 \times 10^6 \gamma^2 B(G) \quad Hz$$

In general p = 2 - 3 in some cases flatter/steeper

ISM B ~ 3×10^{-6} G ν up to ~ 5 GHz $\gamma \sim 10^3$-10^4

Questions: 1. Origin of NT electrons (and cosmic rays in general)
2. Why different p:s in different sources and at different frequencies

Longair 19.2

Energy losses of relativistic electrons

Ionization losses

$$\frac{dE}{dt} = 7.6 \times 10^{-9} n_{HI} (3 \, ln \, \gamma + 19.8) \quad eV \; s^{-1}$$

$$\tau = \frac{E}{dE/dt} \propto E$$

Bremsstrahlung = free-free

Ionized (H II)

$$\frac{dE}{dt} = 4 n_p Z^2 \alpha r_e^2 c \, g \, E \qquad g = \ln \gamma + 0.36$$

$$\frac{dE}{dt} = 7 \times 10^{-17} n_p (\ln \gamma + 0.36) E(eV) \quad eV \; s^{-1}$$

Neutral (H I)

$$\frac{dE}{dt} = 3.7 \times 10^{-16} n_{HI} E(eV) \quad eV \; s^{-1}$$

$$\tau = \frac{E}{dE/dt} \propto E$$

Synchrotron losses

$$\frac{dE}{dt}=2\sigma_T c\gamma^2 U_B \sin^2\theta$$

Isotropic B-field

$$\frac{1}{2}\int_0^\pi \sin^2\theta\, d\cos\theta=\frac{2}{3}$$

$$\boxed{\frac{dE}{dt}=\frac{4}{3}\sigma_T c\gamma^2 U_B=6.6\times10^{-4}\gamma^2 B^2 \quad eV\ s^{-1}}$$

Inverse Compton

$$\frac{dE}{dt}=\frac{4}{3}\sigma_T c\gamma^2 U_{rad}$$

$$\left.\frac{dE}{dt}\right|_{IC} \Big/ \left.\frac{dE}{dt}\right|_{synch}=\frac{U_{rad}}{U_B}$$

Adiabatic losses

$$\frac{dE}{dt} = -p\frac{dV}{dt}$$

$$\frac{d\rho}{dt} = -\rho\nabla\cdot\boldsymbol{v}$$

$$\rho = \frac{1}{V}$$

$$\frac{dV}{dt} = -V^2\frac{d\rho}{dt} = -V\nabla\cdot\boldsymbol{v}$$

$$E = \frac{pV}{(\gamma-1)}$$

$$\frac{dE}{dt} = -p\frac{dV}{dt} = (\gamma-1)E\nabla\cdot\boldsymbol{v}$$

$$\boxed{\frac{dE}{dt} = -p\frac{dV}{dt} = (\gamma-1)E\,\nabla\cdot\boldsymbol{v}}$$

Important example: Homologous expansion

$$v(r) = v_0\frac{r}{r_0}$$

$$\nabla\cdot\boldsymbol{v} = \frac{1}{r^2}\frac{\partial}{\partial r}(r^2 v) = \frac{v_0}{r_0}\frac{1}{r^2}\frac{\partial}{\partial r}(r^3) = 3\frac{v_0}{r_0} = 3\frac{v}{r}$$

$$\boxed{\frac{dE}{dt} = 3(\gamma-1)E\frac{v}{r} = 3(\gamma-1)\frac{E}{t} = \frac{E}{t}}$$

relativistic $\gamma=4/3$

Diffusion losses

Longair 19.3

Assume that the electrons scatter against magnetic field irregularities ⇒ diffusion in space

Consider the change in a volume in an energy – space volume dE dx

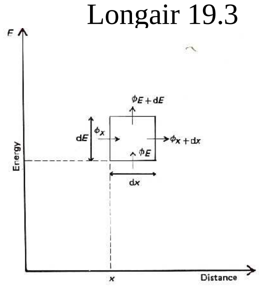

$$\frac{dn(E,x,t)}{dt}dE\,dx=[\phi_x(E,x,t)-\phi_x(E,x+dx,t)]dE$$
$$+[\phi_E(E,x,t)-\phi_E(E+dE,x,t)]dx+Q(E,x,t)dE\,dx$$

source

$$\frac{dn(E,x,t)}{dt}=-\frac{\partial\phi_x(E,x,t)}{\partial x}-\frac{\partial\phi_E(E,x,t)}{\partial E}+Q(E,x,t)$$

Diffusion through dE .

diff. coeff.

$$\phi_x(E,x,t)=-D\frac{\partial n(E,x,t)}{\partial x}$$

Diffusion losses II

$$\frac{dn(E,x,t)}{dt} = D\frac{\partial^2 n(E,x,t)}{\partial x^2} - \frac{\partial \phi_E(E,x,t)}{\partial E} + Q(E,x,t)$$

$$\boxed{\frac{dn(E,x,t)}{dt} = D\nabla^2 n(E,x,t) - \frac{\partial \phi_E(E,x,t)}{\partial E} + Q(E,x,t)}$$

$$\phi_E(E,x,t) = n(E)\frac{dE}{dt} = -b(E)n(E)$$

$$\boxed{\frac{dn(E,x,t)}{dt} = D\nabla^2 n(E,x,t) + \frac{\partial}{\partial E}[b(E)n(E,x,t)] + Q(E,x,t)}$$

Diffusion losses III

Assume steady state, uniform source distribution, infinite extent

$$\frac{d}{dE}[b(E)n(E)] = -Q(E)$$

$$\int d[b(E)n(E)] = -\int Q(E)\,dE$$

$$b(E)n(E) = \int_E^{\infty} Q(E)\,dE \qquad if\ n(\infty) \to 0$$

$$\boxed{n(E) = \frac{\kappa E^{-(p-1)}}{(p-1)\,b(E)}}$$

$$\boxed{b(E) = A_1(\ln E/m_e c^2 + 19.8) + A_2 E + A_3 E^2}$$

ionization adiab., free-free synchro / IC

Longair 19.5

Minimum energy argument

Suppose we have a radio source with luminosity L_ν.
What is the magnetic field and energy density?

$$\frac{dn}{dE} = \kappa E^{-p}$$

$$L_\nu = A(\alpha) V \kappa B^{1+\alpha} \nu^{-\alpha} \qquad \alpha = (p-1)/2$$

$$W = V\left(\epsilon_e + \epsilon_p + \frac{B^2}{8\pi}\right)$$

$$\epsilon_e + \epsilon_p \equiv \eta \epsilon_e$$

$$W = V\left(\epsilon_e \eta + \frac{B^2}{8\pi}\right) = V\left(\int_{E_{min}}^{E_{max}} \kappa E^{-p} E \, dE + \frac{B^2}{8\pi}\right)$$

$$W = V\,(\epsilon_e \eta + \frac{B^2}{8\pi}) = V\,(\int_{E_{min}}^{E_{max}} \kappa\, E^{-p}\, E\, dE + \frac{B^2}{8\pi})$$

$$\nu_{max} = 0.29\,\nu_c = 0.29 \cdot 4.2 \times 10^6\, \gamma^2\, B(G) = 1.2 \times 10^6\, \gamma^2\, B(G) \equiv C\, E^2\, B$$

$$W_e = V \int_{E_{min}}^{E_{max}} \kappa\, E^{-p+1} dE = V\, \frac{\kappa}{(p-2)} (E_{min}^{-p+2} - E_{max}^{-p+2})$$

$$W_e = V\, \frac{\kappa (C\, B)^{(p-2)/2}}{(p-2)} [\nu_{min}^{-(p-2)/2} - \nu_{max}^{-(p-2)/2}]$$

$$W_e = V \frac{\kappa (C B)^{(p-2)/2}}{(p-2)} [\nu_{min}^{-(p-2)/2} - \nu_{max}^{-(p-2)/2}]$$

$$L_\nu = A(\alpha) V \kappa B^{1+\alpha} \nu^{-\alpha}$$

$$W_e = \frac{V (C B)^{(p-2)/2}}{(p-2)} \frac{L_\nu}{A(\alpha) V B^{1+\alpha} \nu^{-\alpha}} [\nu_{min}^{-(p-2)/2} - \nu_{max}^{-(p-2)/2}]$$

$$\alpha = (p-1)/2$$

$$W_{part} = \eta G(\alpha, \nu_{min}, \nu_{max}) L_\nu B^{-3/2} \nu^{\alpha}$$

$$W_{tot} = \eta G L_\nu B^{-3/2} \nu^{\alpha} + V \frac{B^2}{8\pi}$$

$$W_{tot} = \eta\, G\, L_\nu\, B^{-3/2} \nu^\alpha + V \frac{B^2}{8\pi}$$

$$B_{min} = \left[\frac{6\pi\, \eta\, G\, L_\nu\, \nu^\alpha}{V} \right]^{2/7}$$

$$W_{min\, B} = V \frac{B^2}{8\pi} = \frac{3}{4} W_{min\, part}$$

$$W_{min\, tot} = \frac{7}{4} \frac{V^{3/7}}{8\pi} \left[6\pi\, \eta\, G\, L_\nu\, \nu^\alpha \right]^{4/7}$$

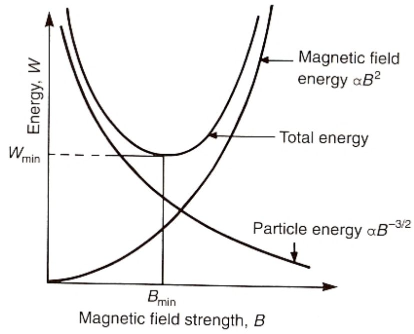

1. There is no obvious physical reason why the magnetic field and particle energies should adjust to this minimum energy requirement!

2. For $B = B_{min}$ we have $W_B \sim W_{part}$. Minimum energy field often called equipartition field

3. $W_{min\ tot}$ is a strict lower limit to the total energy.

4. $W_{min\ tot}$ is sensitive to the non-thermal proton/electron ratio. This can be large, but is not directly observable.

5. W_{part} depends on the minimum energy (for $\alpha > 0.5$, or $p > 2$). ν_{min} is difficult to determine from observations.

6. W depends on the emitting volume. Filling factor may be low!

Practical formulae

Assume a typical spectral index α=0.75, i.e. p=2.5.
Minimum energy $\nu_{min} = \nu$.

$$B_{min} = 1.8 \times 10^4 \left[\frac{\eta L_\nu}{V} \right]^{2/7} \nu^{1/7} \quad G$$

$$W_{min\,tot} = 3 \times 10^{13} V^{3/7} \left(\eta L_\nu \right)^{4/7} \nu^{2/7} \quad erg$$

Ex. Cygnus A

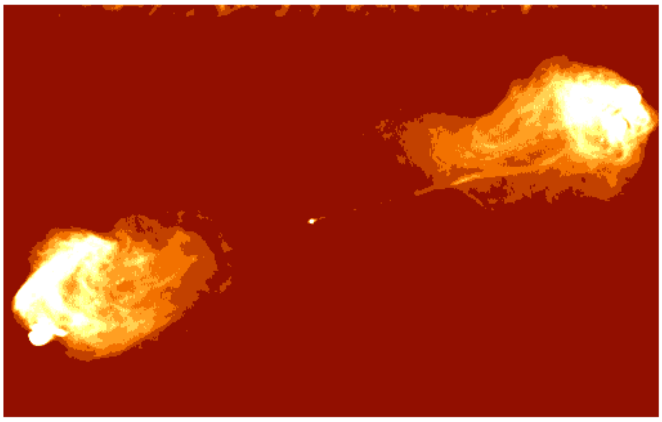

$$R \approx 50\,kpc = 1.5 \times 10^{23}\,cm \qquad L_\nu \approx 8 \times 10^{35}\,erg/s/Hz \quad at\ 178\ MHz$$

$$W_{min\ tot} = 2 \times 10^{59}\,\eta^{4/7}\ \ erg \ = \ 3 \times 10^{5}\,M_O c^2$$

Supernova remnants

Chandra X-rays 0.5-8 keV

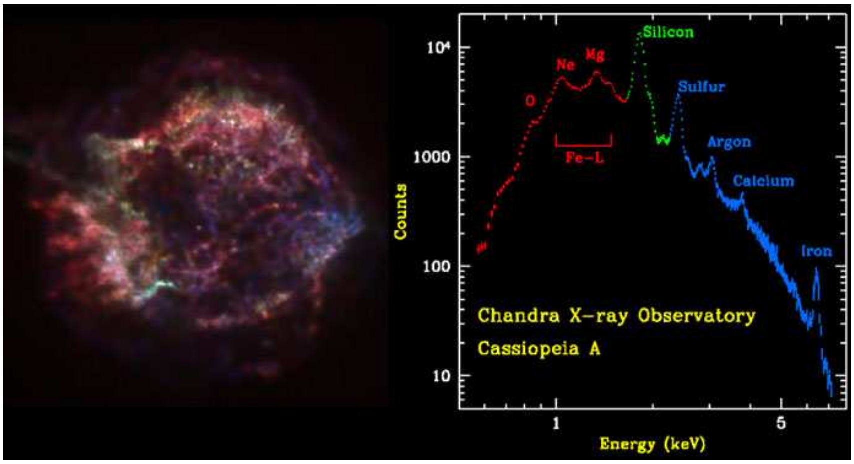

Thermal spectrum: Line emission + free-free continuum

Left: Cas A. This is the result of the explosion of a massive star, ~ 20 - 40 $M_{\odot}$, approximately 1672. The spherical shape of the remnant shows that it is interacting with a fairly uniform circumstellar medium. Ejecta shows considerable structure resulting from hydrodynamical instabilities during the explosion.

Right: Spectrum dominated by thermal emission from many atomic lines. Continuum from free-free emission.

VLA radio 8.4 GHz

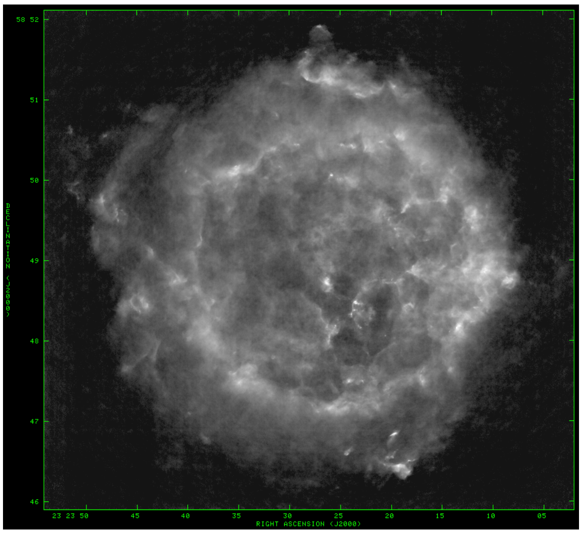

$F_\nu \propto \nu^{-\alpha}$ young SNRs $\alpha \approx 0.8$ old $\alpha \approx 0.5$

Radio image of Cas A reflecting the magnetic field and non-thermal electron distribution.

The spectrum is well described by a power law. For young remnants, like Cas A, this is fairly steep with spectral index ~ 0.8, while more evolved have a spectral index close to 0.5.

Expanded version of L 19.4

Expansion of a point explosion

Assume a spherical, adiabatic expansion in a uniform density medium with no external pressure ⇒ strong shock, constant total energy. Assume that the shell is very thin (to be checked later).

Momentum $$\frac{d}{dt}(M\,v)=4\pi r^2(p-p_{ext})\approx 4\pi r^2 p$$

Mass $$M=\frac{4\pi}{3}r^3\rho$$

In shock frame $$v'_1=-V_s \qquad v'_2=\frac{-V_s}{4}$$

In 'observer' frame $$v=v'-V_s=\frac{3}{4}V_s=\frac{3}{4}\frac{dr}{dt}$$

$$\frac{1}{4}\rho\frac{d}{dt}\left(r^3\frac{dr}{dt}\right)=r^2 p$$

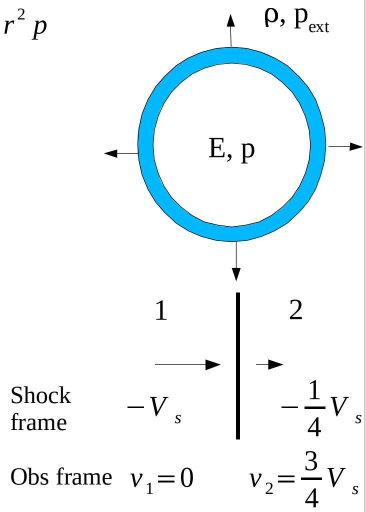

Calculate the evolution of a point explosion in a uniform medium.

If we can neglect the external pressure compared to the internal pressure, which is in general a very good approximation, there are only two free parameters, E and ρ. Further, we neglect the mass of the supernova ejecta in the total mass.

If we further assume that the shell is thin (checked later!) we can neglect the variation of the variables in this and use Newtons equation for the momentum conservation.

To get a relation between the shock velocity and the velocity of the gas in the shell we use the jump conditions.

$$E_{tot} = E_{therm} + E_{kin} = \epsilon V + \frac{1}{2} M v^2 = constant$$

$$\epsilon = \frac{p}{(\gamma - 1)} = \frac{3}{2} p \qquad \gamma = 5/3$$

$$E_{tot} = \frac{3}{2} p V + \frac{1}{2} M v^2$$

$$E_{tot} = \frac{3}{8} \frac{\rho}{r^2} \frac{d}{dt} \left(r^3 \frac{dr}{dt}\right) \frac{4\pi}{3} r^3 + \frac{1}{2} \rho \frac{4\pi}{3} r^3 \left(\frac{3}{4} \frac{dr}{dt}\right)^2$$

$$r = A t^{\alpha}$$

$$E_{tot} = A^5 \frac{\pi}{2} \rho t^{5\alpha - 2} \left[\alpha (4\alpha - 1) + \frac{3}{4} \alpha^2\right]$$

E_{tot} constant $\qquad \alpha = \frac{2}{5}$

$$E_{tot} = A^5 \rho \frac{9\pi}{50}$$

$$\boxed{r = A t^{\alpha} = \left(\frac{50}{9\pi}\right)^{1/5} \left(\frac{E_{tot}}{\rho}\right)^{1/5} t^{2/5} \approx 1.12 \left(\frac{E_{tot}}{\rho}\right)^{1/5} t^{2/5}}$$

Sedov-Taylor similarity solution. Exact similarity solution gives 1.17...

Swept up mass $\quad M = 4\frac{\pi}{3} r^3 \rho = 4\pi r^2 \rho_2 \Delta r$

$$\rho_2 = 4\rho \quad \Rightarrow \quad \boxed{\Delta r = \frac{r}{12}}$$

Thin shell approximation ok!

Note that as we anticipated this solution only depends on E and ρ. The fact that it is a power law solution means that all properties, like density and velocity, only depends on this scaling variable.

Finally, we have to check that the thin shell approximation is a good one. This we do by calculating the mass of the shell which should be equal to that of the swept up mass. Using the jump condition for the density ratio we get the thickness

This solution was used by Taylor and Sedov to estimate the energy of the first American nuclear explosions from the diameter of the cloud from photographs of the explosion.

Behind the shock

$$r = 1.1\left(\frac{E_{tot}}{\rho}\right)^{1/5} t^{2/5} = 1.6\times10^{19} E_{51}^{0.2} n^{-0.2}\left(\frac{t}{1000 \quad yrs}\right)^{0.4} \quad cm$$

$$V_s = \frac{dr}{dt} = \frac{2}{5}\frac{r}{t} = 2.0\times10^{3} E_{51}^{0.2} n^{-0.2}\left(\frac{t}{1000 \quad yrs}\right)^{-0.6} \quad km\, s^{-1}$$

$$\boxed{T = 1.36\times10^{7}\left(\frac{V_s}{1000\, km/s}\right)^{2} = 5.6\times10^{7} E_{51}^{0.4} n^{-0.4}\left(\frac{t}{1000 \quad yrs}\right)^{-1.2} \quad K}$$

The typical energy of a supernova is ~ 10^{51} ergs, and the typical density of the interstellar medium is ~ 1 cm^{-3}. The radius is therefore given by the expression above and is of the order of a few pc after 1000 years.

The velocity of the shock is obtained as the derivative of the shock radius with respect to time, and is a few thousand kilometers at this epoch.

The temperature of the shock is given by the shock conditions, and together with the shock velocity above, is 10^7 – 10^8 K during this time interval. Note the fairly rapid decrease of the temperature with time.

Reverse shock

Pressure from outward shock drives reverse shock back into interior. Separated by contact discontinuity

p ~ constant between shocks

$$\rho_{csm} V_s^2 \approx \rho_{ej} V_{rev}^2$$

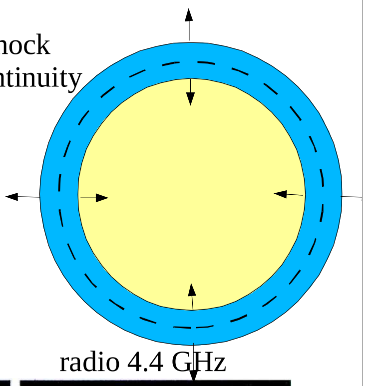

Cas A Si 4-6 keV cont. radio 4.4 GHz

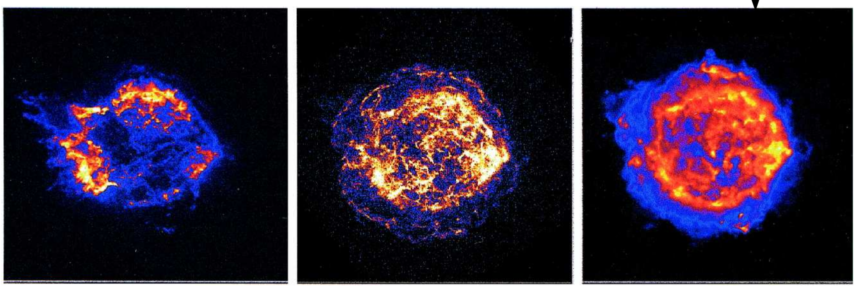

While we neglected the ejecta mass in the Sedov solution it is important for very young remnants, with ages less than ~ 1000 years.

The pressure behind the shock send a reverse shock back into the ejecta, and heats and compresses also this. This shock moves back into the ejecta only in a comoving frame. In the observers frame also this expands, but less rapidly than the external shock. After a few hundred years this reaches the center and heats up the whole remnant.

The reverse shock can be seen clearly as the inner boundary in especially the X-ray and radio continuum images of Cas A

From Supernova to Supernova Remnant

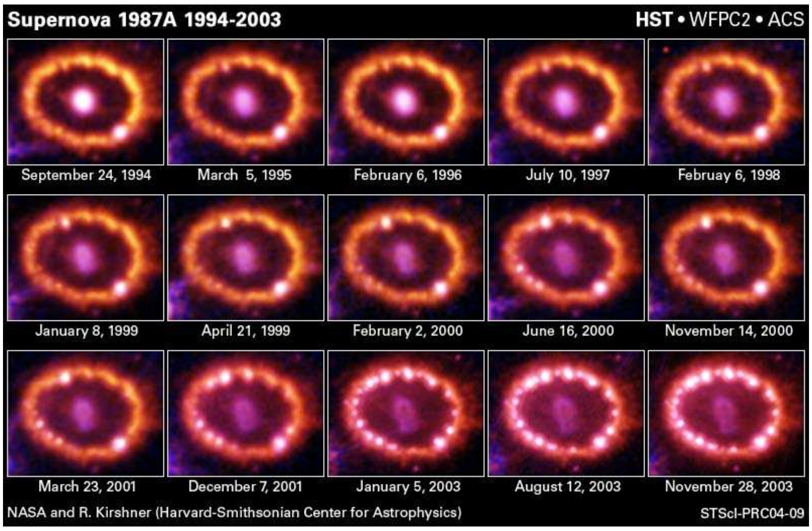

V_{exp} ~ 30,000 km/s; collision with ring after ~ 10 years

This picture of SN 1987A shows both the expansion of the ejecta itself as the blob in the center of the ring. The ring itself was ejected from the supernova progenitor 10,000 years before the explosion, and was heated and ionized by the supernova at the time of the explosion by the first burst of soft X-ray radiation.

The ejecta has now reached the inner parts of the ring and is gradually shocking the gas it encounters, giving rise to these 'hot spots'. I a few years the whole ring will be shocked by the ejecta and finally swept up and evaporated by this.

Thermal emission

X-ray spectrum dominated by thermal emission from the interior

Ionization by collisions. $e + X_i \rightarrow X_{i+1} + e$

Needs energy

$$\frac{1}{2} m_e v^2 \approx k T_e \approx \chi_i$$

$$T_e \approx 1.16 \times 10^4 \chi_i (eV) \quad K$$

Number of ionizations per volume, unit time

$$\frac{dn_i}{dt} = n_e n_i C_i(T_e)$$

Note! In many plasmas dominate photoionisation over collisional.

In many cases the emission from supernova remnants, clusters of galaxies, stellar coronae, active galaxies and other objects is dominated b thermal plasmas, with a Maxwell-Boltzmann distribution for the electrons. The spectra of these are important as diagnostics of the hot plasma.

To calculate the spectrum we first need to calculate the state of ionization. In the simple case that collisional ionization dominates, i.e., ionization by thermal electrons, this is relatively easy to calculate.

In order to ionize an ion i the electrons have to have a thermal energy roughly corresponding to the ionization potential, χ_i. In reality his occurs by the tail of the M-B distribution

Recombination by radiative capture

$$e+X_{i+1}\rightarrow X_i+h\nu$$

$$\frac{dn_i}{dt}=n_e n_{i+1}\alpha_{i+1}(T_e)$$

In steady state

$$n_i C_i(T_e)=n_{i+1}\alpha_{i+1}(T_e)$$

Number conservation

$$\sum_i n_i=n_{tot}$$

Typically

$$C_i(T_e)\propto T_e^{-1/2}e^{-kT_e/\chi_i} \qquad \alpha_{i+1}(T_e)\propto T_e^{-0.7}$$

The ionizations are balanced by recombinations, where free thermal electrons are captured by positive ions.

Balancing these two processes we see that, since they are both proportional to the electron density, this cancels.

In this way we can set up a set of equations describing the ratios of successive ionization stages. These relations together with the requirement that the sum of the different ionization stages should add up to the total number of ions of this element, this gives the solution.

While the ionization rate is very sensitive to the temperature, since it is the M-B tail which is most important, the recombination rate is much less sensitive.

Collisional ionization equilibrium for iron

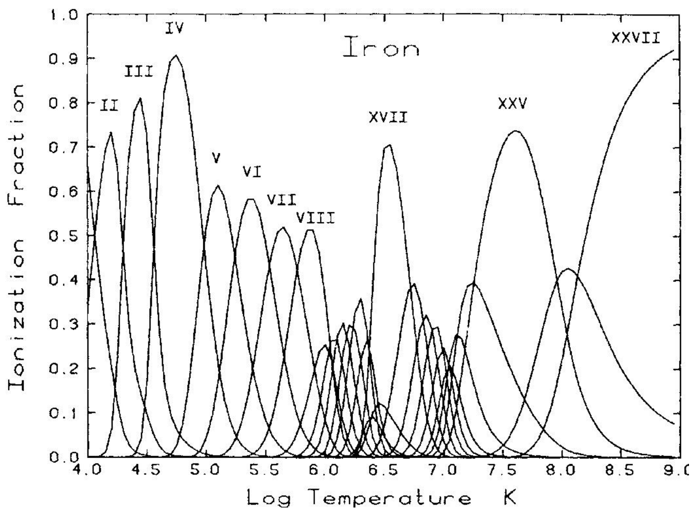

Shull 1979

Because the electron density cancels the ionization equilibrium is only a function of temperature, and can therefore be calculated under very general conditions. This is in contrast to a situation where photoionization is important.

This plot shows the fraction of the ions of the different ionization stages for iron as function of temperature. In the temperature range where X-ray emission is important, it is seen that the important ions are Fe XVII at ~ 10^6-10^7 K, and Fe XXIV-XXVI form 10^7-10^8 K.

Thermal emission

X-ray spectrum dominated by thermal emission from the interior

Continuum radiation: Free-free emission

$$\frac{dE}{d\nu\, dt\, dV} = n_e n_i \frac{C}{T_e^{0.5}} e^{-h\nu/kT_e}$$

$$\frac{dE}{dt\, dV} = n_e n_i \Lambda(T_e) \propto n_e n_i T_e^{0.5}$$

Line emission: Collisional excitation of discrete levels i ➔ j followed by radiative decay j ➔ i

$$\frac{dE_{ij}}{dt} = n_e n_i h\nu_{ij} \frac{\Omega_{ij}}{g_i T_e^{0.5}} e^{-h\nu_{ij}/kT_e}$$

$\Omega_{ij} =$ collision strength

$g_i =$ stat. weight of level i

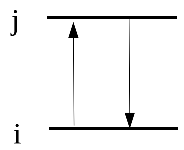

Given the ionization state, we can now calculate the emission from the plasma. This consists of continuum radiation and line emission.

The most important continuum source above 10^7 K is free-free emission. This has a characteristic exponential spectral shape from the Boltzmann factor, which is important as a temperature diagnostic of a plasma.

The line emission is dominated by collisional excitation, followed usually by radiative de-excitation. The rate is again determined by the MB-factor and a quantity, the collision strength Ω, which depends on the atomic parameters of the transition.

Cooling function

$$-\frac{dE}{dV\,dt}=n_e n_i \Lambda(T_e)$$

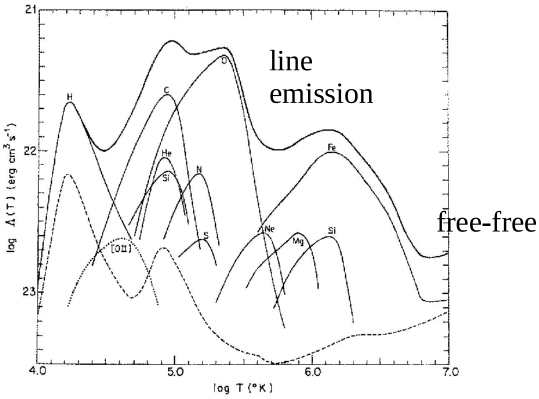

$T_e > 10^7$ K: Free-free emission dominates cooling

$T_e < 10^7$ K: Line emission dominates cooling

$$\boxed{\Lambda(T_e)=8.0\times10^{-23}(Z/Z_O)\left(\frac{T_e}{10^6 K}\right)^{-0.90}+2.3\times10^{-24}\left(\frac{T_e}{10^6 K}\right)^{0.50}\quad erg\ \ cm^3\ \ s^{-1}}$$

When we add up all sources of emission, lines and continuum, and integrate over all wavelengths, this gives the total cooling rate of the plasma. Because all processes, both ionization, recombination, and emission processes, are proportional to the electron density and the ion density, we can factor out this and define a cooling function which is only dependent on temperature.

The figure shows that line emission of successively heavier elements up to ~ 10^7 K, when free-free radiation takes over. The cooling function has therefore a minimum at ~ 10^7 K. The expression below is a useful approximation for many situations.

Shock spectra for different shock temperatures

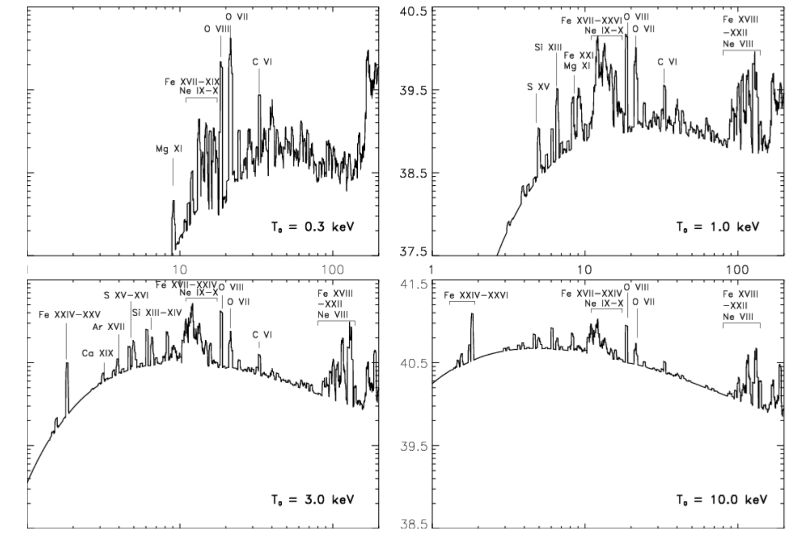

T. Nymark 2005)

These panels show examples of spectra from a shock wave with different temperature (and therefore velocity) behind the shock. The most important thing to note is the change in the spectrum from a continuum dominated at 10 keV (108 K), to a more and more line dominated. At 3 keV the Fe K line at 7 keV is strong. At lower temperature emission lines of lower ionization stages, like Fe XVII, and lower atomic number become more and more important.

Cas A

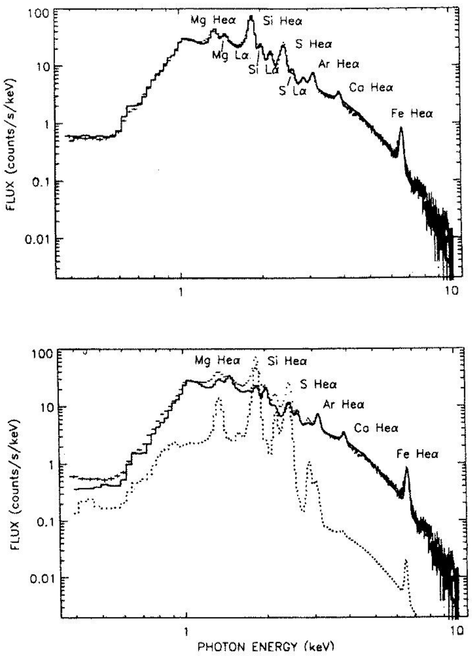

X-ray spectrum of Cas A, showing a thermal continuum due to free-free emission and many lines of different elements.

The modeling of these spectra give important information about the abundances of the newly created elements, as well as the physical parameters, like density and temperature.

red = Si Heα (1.78–2.0 keV), blue = Fe K (6.52–6.95 keV), and green = 4.2–6.4 keV continuum.

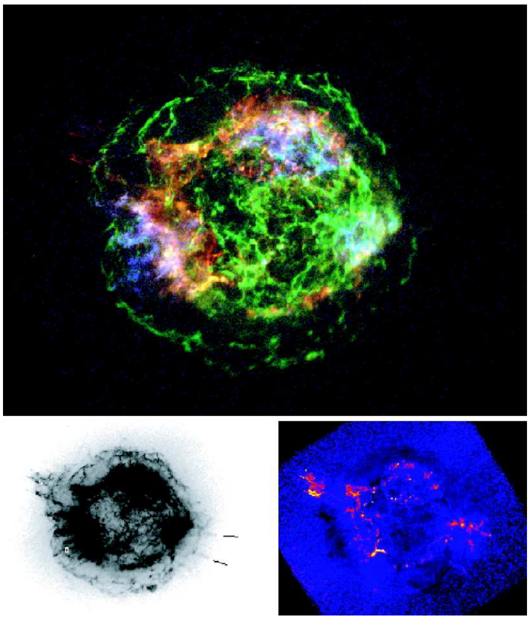

Image of Cas A in several energy bands. In the 1.78-2.0 keV band (red) silicon dominates the emission, in the 6.52-6.95 keV band iron, and in the 4.2-6.4 keV continuum emission.

The different bands show the spatial distribution of the newly processed material. Somewhat unexpected iron is not only seen at the center but at very high velocities (i.e., large radii).

Tycho's remnant = SN 1572

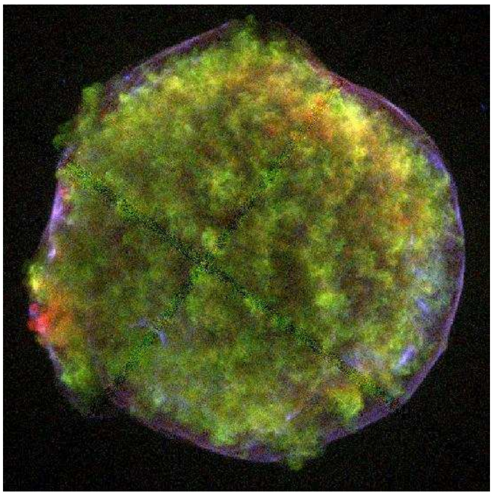

Chandra (Warren et al 2005)

Interior dominated by thermal emission.

Thin rim dominated by continuum probably synchrotron

Shock acceleration?

Image of Tycho's remnant with Chandra. In contrast to Cas A this was the result of a Type Ia supernova.

The interior is dominated by thermal emission from iron and intermediate mass elements like Si. The thin outer blue rim shows continuum emission from non-thermal electrons which radiate synchrotron emission. This is most likely due to freshly accelerated electrons at the outer shock wave.

Radiative stage

Thermal instability ⇒ cooling to ~ 10^4 K ⇒
Optical line emission Hα, [O III] etc
p ~ constant ⇒ $n \propto T^{-1}$

$$\frac{d}{dt}(M\,v)=4\pi\,r^2(p-p_{ext})\approx 0$$

$$M=\frac{4\pi}{3}r^3\rho$$

$$\frac{d}{dt}(r^3 v)=0$$

$$r^3 v = constant$$

$$r = A\,t^{1/4}$$

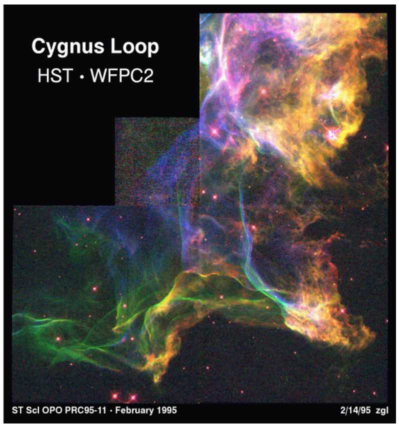

v ~ 115 km s^{-1}
20 pc diameter
X-rays below ~ 2 keV

Because the temperature is decreasing $T \propto t^{-1.2}$, (see earlier slide), the temperature will fall below 10^7 K after a few thousand years. The cooling then increases with decreasing temperature and a cooling run-away will occur. The cooling will continue until T ~ 10^4 K, when photoionization by radiation balances heating. Instead of X-rays, the plasma will then emit mainly optical emission in lines like Hα and O III.

In this stage the energy is obviously not longer conserved behind the shock. We can then approximate the dynamics by a momentum conserving shell, which sweeps up mass like a snow plow.

A nice example of a remnant in this phase is the Cygnus Loop which has an age of ~ 40,000 years.

Clusters of galaxies

Coma

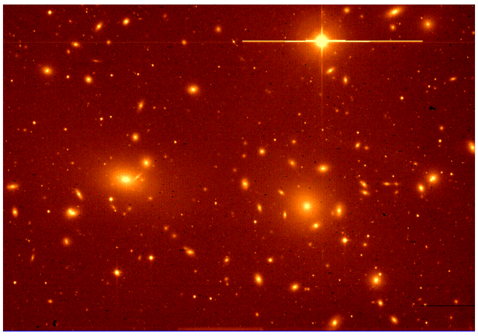

100-1000 galaxies

Velocity dispersions (line of sight)
400-1400 km/s

Mass $10^{14} – 3x10^{15}\ M_O$

Radius ~ 1.5-3 Mpc

M/L ~ 200-300 M_O/L_O

Gas/stellar mass 2-10

$L_x \sim 10^{43} – 10^{45}$ erg/s

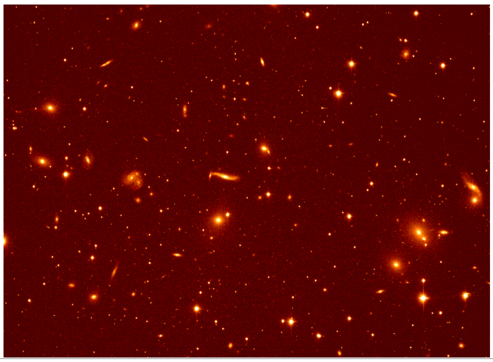

Hercules

Clusters of galaxies have high energy properties fairly similar to supernova remnants.

Physically these are the largest bound systems containing 100-1000 galaxies. The velocity dispersion is 400-1500 km/s.

These are strong sources of X-rays from hot gas and the most interesting aspect of this is that this gas is a very useful probe of both the gas itself and especially the cluster mass distribution, in particular the dark matter.

The upper image shows an optical image of the Coma cluster which is the nearest massive cluster.
The galaxy distribution is dominated by old ellipticals and is smooth. The lower image is the Hercules cluster which has a more irregular distribution and a large fraction of young spirals.

X-ray emitting gas in clusters of galaxies

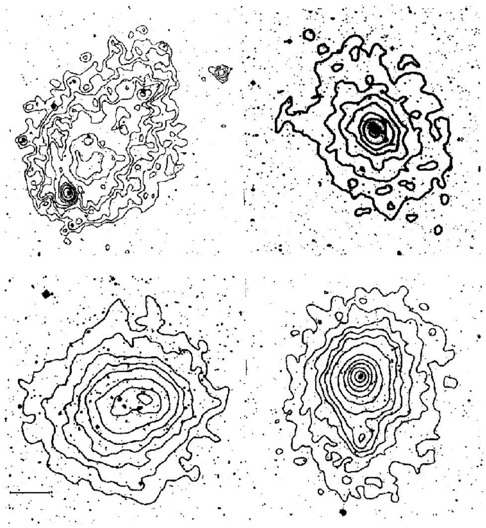

These images show four clusters in X-rays and optical. The X-ray emission is shown by the contours. Three of these are relaxed, showing a smooth centrally concentrated emission, while the upper left has a more irregular appearance

Scalings

Virial equilibrium of gas and matter

$$\boxed{L_X \approx V\, n_e^2 \Lambda \propto n_e^2 R^3 T_e^{1/2}}$$

$$k\,T_e \approx \sigma^2 \approx \frac{GM_{tot}}{R}$$

$$n_e \approx \frac{M_{gas}}{V} \propto \frac{M_{tot}}{R^3} \propto \frac{T_e}{R^2}$$

$$\boxed{L_X \propto n_e^2 (T_e / n_e)^{3/2} T_e^{1/2} = n_e^{1/2} T_e^2}$$

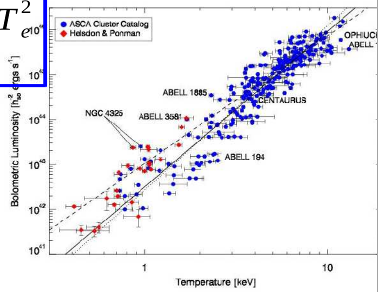

Observationally there is a tight correlation between the X-ray derived temperature of the gas and the velocity dispersion of the galaxies, as is expected if the cluster is in virial equilibrium.

The X-ray luminosity of cluster is determined by the volume averaged density and cooling rate. Together with the temperature – velocity dispersion relation and the density we get a scaling relation between the X-ray luminosity and temperature, which is a check on the relaxed state of the cluster.

This agrees well with the observations.

Observe surface brightness, S, as function of projected radius R

$$S(R)=2\int_0^{\infty} n_e(l)^2\,\Lambda[T(l)]\,dl=2\int_R^{\infty}\frac{n_e(r)^2\,r\,\Lambda[T(r)]}{(r^2-R^2)^{1/2}}dr$$

$$n_e(r)=n_0\left[1+\left(r/R_c\right)^2\right]^{-3\beta/2}$$

$$\Lambda[T]\approx 2.4\times 10^{-27}\,T^{1/2}\qquad t>2\times 10^7\,K$$

Spectrum $\Rightarrow$ T(r). Typically $10^7 < T_e < 10^8$

Make fit to S(R) $\Rightarrow$ β, n_0, R_c.

$R_c \sim 0.15 - 0.4$ Mpc $\quad \beta \sim 0.7 \quad n_0 \sim 2.5\text{x}10^{-3}\ \text{cm}^{-3}$

Using observations of the line f sight integrated surface brightness, S, as function of the projected cluster radius R, one can derive an expression for the integrated electron density and temperature.

For T > 10^7 free-free emission dominates. A fit to the surface brightness then gives the density as function of radius.

An example: Abell 478 with Chandra and XMM

Surface brightness

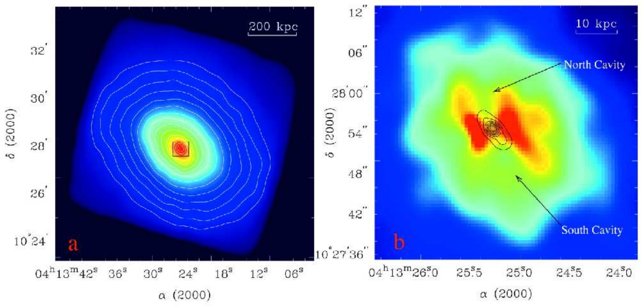

Hardness 2-5 keV/0.5-2 keV

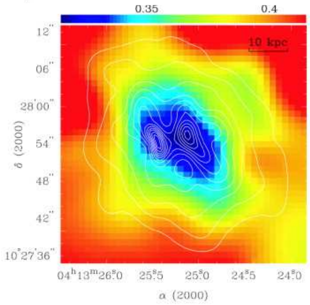

As an example we consider the cluster Abell 478. The X-ray distribution is smooth, showing that the cluster is well relaxed.

From the hardness ratio in the lower panel one sees that the cluster is clearly cooler in the center.

Surface brightness, density, temperature & pressure

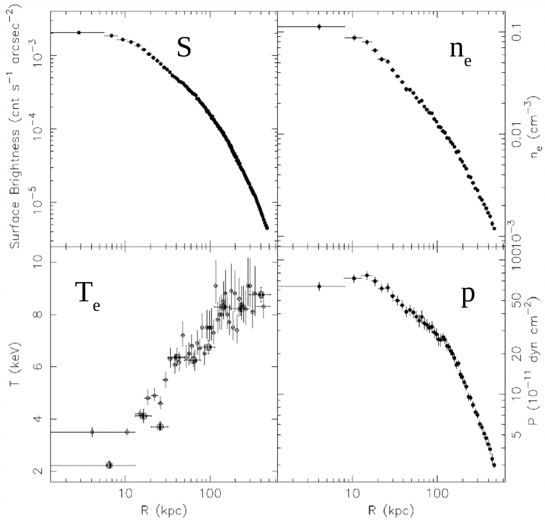

T decreases at center: Cooling flow

These panes show the observed surface brightness in the upper left panel. The lower left shows the temperature distribution as function of radius, showing more quantitatively that the temperature is considerably lower in the center.

From these the density in the upper right panel is derived, and the pressure then follows.

$$\frac{dp}{dr} = \frac{-G\,M(r)\rho(r)}{r^2}$$

$$p = \frac{k}{m_p \mu} \rho\, T$$

$$\frac{dp}{dr} = \frac{k}{m_p \mu} \left(T \frac{d\rho}{dr} + \rho \frac{dT}{dr}\right)$$

$$\boxed{M(r) = \frac{-k\,r\,T}{G\,m_p \mu} \left(\frac{d \ln \rho}{d \ln r} + \frac{d \ln T}{d \ln r} \right)}$$

T(r) and n_e(r) from spectrum and surface brightness ⇒ mass distribution.
Note: This is the total mass, not only the mass in the gas.

Useful probe of the dark matter distribution in the cluster.

Assuming that the cluster gas is in equilibrium we have the usual hydrostatic equation for the gas pressure and the gravitational force. Note here, however, that the mass is not only he gas mass but the total mass, including dark matter.

This equation can be written in a form where the right hand side have only quantities derivable from the observations, as we have just showed. Therefore we can from these observations derive the total cluster mass as function of radius.

Total mass distribution

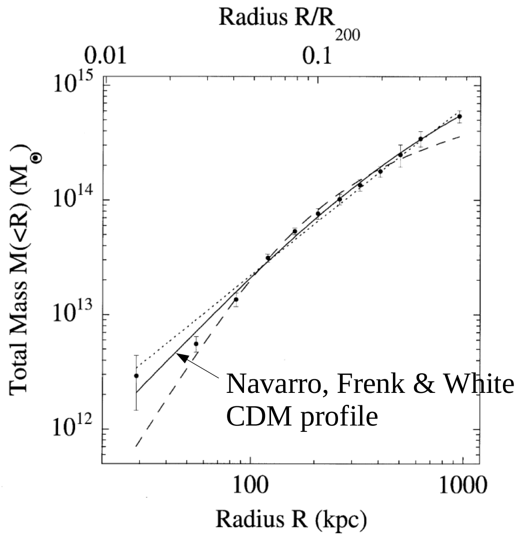

Total mass 1×10^{15} M_O, gas fraction 13 %.

This plot shows the result for Abell 478, which shows that he total mass, as far as one can trace the X-rays (~ 1 Mpc), is ~ 10^{15} M_O.

The mass distribution can be compared to models, as shown by the different lines. One finds that the Navarro-Frenk-White distribution, which is a result of N-body simulations, gives a very good fit over the whole range.

This shows the usefulness of the X-ray observations as a diagnostic of the dark matter.

Chemical enrichment

Perseus cl.

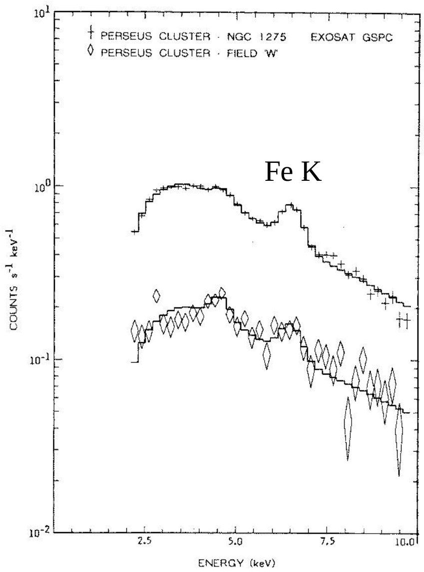

Coma cl.

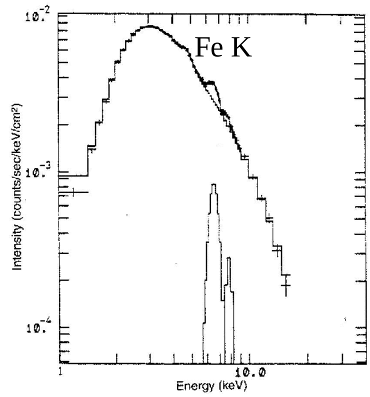

Metalicity ~0.3 times solar +/- 0.1

Outflows from galaxies!

Another important result one derives from X-ray observations concerns the abundances of the heavy elements in the cluster. Spectra of a large number of clusters show that the metallicity (total heavy element abundance) is about 30 % of the solar value.

While smaller than the sun and Milky Way, this is much higher than in old stars in e.g. globular clusters or in the halo of the Milky Way. his shows that the gas in the cluster can not just be primordial but has to be enriched by metals from the stars in the galaxies. This is most likely the result of winds resulting from supernovae in the galaxies and sweeping of the galaxy gas by the gas in the cluster.

Cooling flows

Cooling time

$$t_{cool} \approx \frac{3kT_e}{n_e \Lambda(T_e)}$$

$$t_{cool} \approx 8.5 \times 10^{10} \left(\frac{n}{10^{-3}\, cm^{-3}}\right)^{-1} \left(\frac{T}{10^8\, K}\right)^{1/2} \quad yrs$$

If $t_{cool} < t_{Hubble} \Rightarrow$

Thermal instability $\Rightarrow$ cooling to ~ 10^4 K, pressure decrease

Optical line emission, star formation in center

Heating by central AGN or conduction may prevent instability

The cooling time of the gas is dominated by free-free cooling. This depends as always inversely on the density. For densities higher than ~ 10^{-3} cm^{-3} and lower temperatures the cooling time can be less than the Hubble time.

If this is the case the gas will cool and if this leads to temperatures less than ~ 10^7 K the gas can cool to ~10^4 K in the same way as for the supernova remnants. Optical emission is also seen in the centers of several clusters. Abell 478 earlier showed a clear decrease of the temperature in the center. If this occurs fast, the pressure will also decrease and a flow of the gas to the center may take place. This is known as a cooling flow.

The extent to which this takes place is, however, uncertain and depends on the presence of e.g., other heating sources such as AGNs and conduction.

Sunyaev-Zeldovich effect

Hot gas T ~ 10^8 K $\Rightarrow$ electron scattering $\Rightarrow$ Compton boosting of CMBR

$$\frac{\Delta\nu}{\nu} = \frac{kT_e}{m_e c^2}$$

Compton y-parameter $\boxed{y = \int \frac{kT_e}{m_e c^2} n_e \sigma_T \, dl}$

Intensity change $\propto$ y

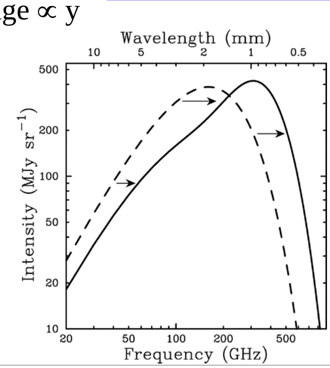

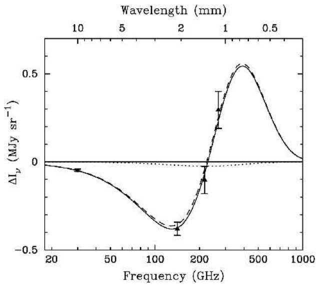

The hot gas in the cluster can scatter radiation coming from behind, leading to a distortion of the spectrum. In particular, the cosmic microwave background radiation will be scattered up to higher frequencies. The extent of this depends on the temperature relative to the electron mass ($m_e c^2$ corresponds to 5×10^9 K) and the optical depth (probability) for scattering, $n_e \sigma_T$ dl.

This is usually combined into the y-parameter which gives the integrated value of this.

The lower panel shows how the scattering results into a decrease of the intensity at frequencies below the intensity peak and to an increase above the peak.

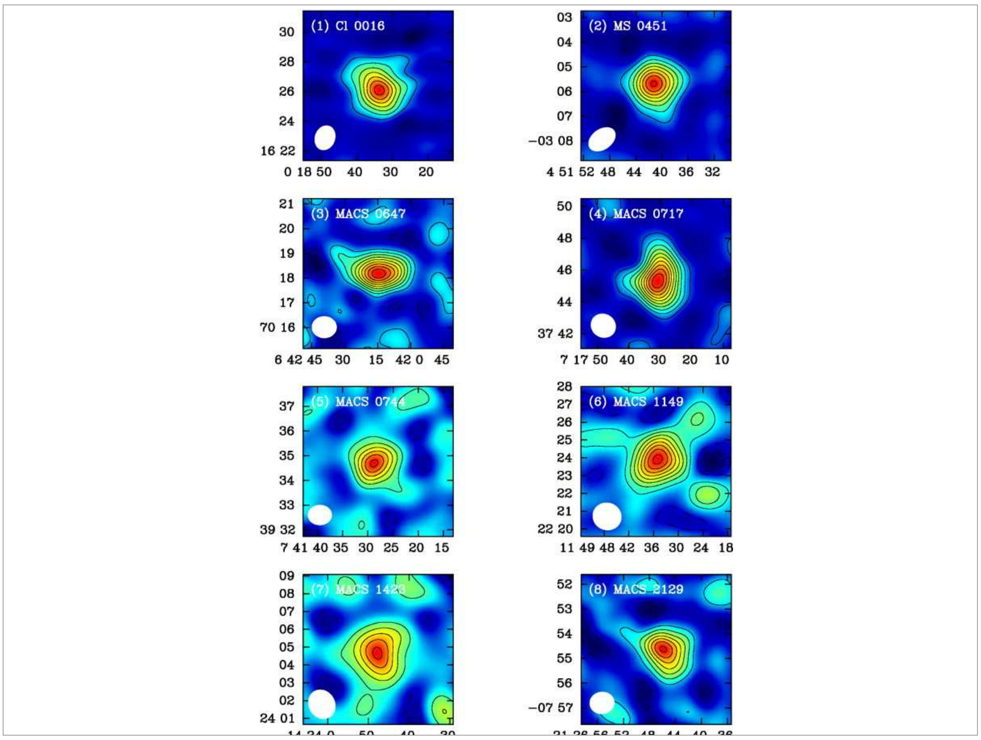

A few clusters showing the intensity change of the CMBR as observed with a millimeter array.

Cosmology with the S-Z effect

Distortion of CMBR gives $$y = \int \frac{kT_e}{m_e c^2} n_e \sigma_T \, dl$$

X-rays give $$F_X = \frac{L_x}{4\pi D^2} = \frac{1}{4\pi D^2} \int n_e^2 \Lambda(T_e) \, dV = \frac{C}{4\pi D^2} \int n_e^2 T_e^{0.5} \, dV$$

+ T_e and θ $$R = \theta D$$

Can determine D i.e., Hubble constant H_0! Result H_0 = 60 km/s/Mpc

Systematic error ~ 30 %

An observational determination of the y-parameter, the cluster temperature from the X-rays and the density from the surface brightness together give an over determined system of relations. These can be used to determine the absolute distance of the cluster, and therefore the Hubble constant.

This has been used for several clusters and the dispersion between the different measurements is only a few percent. The systematic effects are, however, larger and the method can not be compared to e.g. Cepheids or Type Ia supernovae.

Second order Fermi acceleration

Transform from rest system, K, to scattering system K'

$$p'_{x\,1} = \gamma(p_{x\,1} + \frac{V}{c^2} E_1)$$

$$E'_{x\,1} = \gamma(V\,p_{x\,1} + E_1)$$

Suppose scattering is elastic in K', i.e. $E_2' = E_1'$ and $p_2' = -\,p_1'$

Transform back to rest system, K

$$E_2 = \gamma(-V\,p'_{x\,2} + E'_2) = \gamma(V\,p'_{x\,1} + E'_1)$$

$$E_2 = \gamma(V\,\gamma(p_{x\,1} + \frac{V}{c^2} E_1) + \gamma(V\,p_{x\,1} + E_1))$$

particle velocity

$$E_2 = \gamma^2 E_1[1 + 2\frac{V\,p_{x\,1}}{E_1} + \frac{V^2}{c^2}] = \gamma^2 E_1[1 + 2\frac{V\,v\cos\theta}{c^2} + \frac{V^2}{c^2}]$$

Suppose the particle is relativistic (v ~ c) and that the scatterer is non-relativistic (V << c). Then

$$E_2 = \gamma^2 E_1 [1 + 2\frac{v V \cos\theta}{c^2} + \frac{v^2}{c^2}] \approx E_1 [1 + 2\frac{V \cos\theta}{c} + O(V/c)^2]$$

Scattering rate proportional to the flux, F,

$$F = n(v + V \cos\theta) \approx n(c + V \cos\theta)$$

Total change in energy per sec

$$F \Delta E = n(c + V \cos\theta) E_1 \frac{2V \cos\theta}{c}$$

Suppose same number of scatterers with velocities in all directions.
Net increase from each direction (i.e. averaging over the two opposite directions)

$$\Delta E_{net} = n[(c + V\cos\theta)E_1 2V\cos\theta - (c - V\cos\theta)E_1 2V\cos\theta]$$

or

$$\Delta E_{net} = 4n(V\cos\theta)^2$$

Take an average over all directions

$$\boxed{\Delta E_{net} = \frac{\int_0^{\pi/2} 4\frac{n}{c}(V\cos\theta)^2 d\cos\theta}{\int_0^{\pi/2} d\cos\theta} = \frac{4}{3}nc\left(\frac{V}{c}\right)^2}$$

Increase is second order in V/c and is a result of the higher probability for a head-on collision compared to a head-tail collision.

First order Fermi acceleration

Assume that scattering is isotropic in fluid frame

Transform from pre-shock to post-shock where scatt. is elastic

$$E' = \gamma (V\ p_x + E)$$

frame of pre-shock	0	$\leftarrow$ 3/4 V_s
frame of post-shock	3/4 V_s $\rightarrow$	0

V = relative velocity = 3 V_s/4. V << c,

particles relativistic $p_x \sim E/c \cos\theta$

$$E' \approx \frac{V}{c} \cos\theta\, E + E$$

$$\Delta E = \frac{V}{c} \cos\theta\, E$$

$$E(k)=(1+\frac{\Delta E}{E})E(k-1)=.....=(1+\frac{V_s}{c})^k E_0$$

$$N(k)=N_0 P^k$$

$$\ln[N(E)/N_0]=k\ln P=\frac{\ln P\ln[E/E_0]}{\ln(1+\frac{V_s}{c})}$$

$$\frac{N(E)}{N_0}=\left[\frac{E}{E_0}\right]^{\frac{\ln P}{\ln(1+\frac{V_s}{c})}}$$

$$\frac{dN}{dE}=\left[\frac{E}{E_0}\right]^{\frac{\ln P}{\ln(1+\frac{V_s}{c})}-1}$$

Average over angle

Number of crossings per second over shock (normalized)

$$dn = \cos\theta \, d\,\Omega = 2\cos\theta \, d\cos\theta$$

$$\Delta E = \frac{V}{c}\cos\theta \, E$$

$$\left\langle \frac{\Delta E}{E} \right\rangle = 2\int_0^{\pi/2} \frac{V}{c}\cos\theta\cos\theta \, d\cos\theta = \frac{2}{3}\frac{V}{c}$$

2 scatterings per cycle

$$\left\langle \frac{\Delta E}{E} \right\rangle = \frac{4}{3}\frac{V}{c} = V_s$$

Number of crossings per second over shock

$$\frac{dn}{dt} = N\,c\,\frac{1}{2}\int_0^{\pi/2} \cos\theta \, d\cos\theta = \frac{N\,c}{4}$$

only half have positive velocity

Advection rate downstream

$$\frac{dn}{dt} = N\,V = \frac{N\,V_s}{4}$$

Escape probability

$$P_{esc} = \frac{V_s}{c}$$

Scattering prob.

$$P_{scatt} = 1 - P_{esc} = 1 - \frac{V_s}{c}$$

$$\frac{dN}{dE} = C\,E^{\frac{\ln P}{\ln\left(1+\frac{V_s}{c}\right)}-1}$$

$$\frac{\ln P}{\ln\left(1+\frac{V_s}{c}\right)} - 1 = \frac{\ln\left(1-\frac{V_s}{c}\right)}{\ln\left(1+\frac{V_s}{c}\right)} - 1 \approx -1-1=-2$$

$$\boxed{\frac{dN}{dE} = C\,E^{-2}}$$

Note:

- Assumes scattering centers. Alfven waves, magnetic irregularities.....
- Power law depends on compression ratio. In general p = (r+2)/(r-1), where r = 4 for γ =5/3, so p = 2.
- Cosmic rays can give additional pressure and energy loss and modify shock. Usually fattens spectrum (smaller p).
- Relativistic shocks gives smaller p
- Can only accelerate particles to energies where gyroradius up to energies for which the gyroradius is smaller than the size of the object. For cosmic rays this is ~ 10^{14} - 10^{15} eV
- Most of the acceleration of the cosmic rays and electrons assumed to be in supernova remnants for energy reasons. Up to ~ 10^5 years